A Time-Domain Method for Separating Incident and Reflected Irregular Waves

Frigaard, Peter; Brorsen, Michael

Publication date:
1993

Document Version
Publisher's PDF, also known as Version of record

Link to publication from Aalborg University

Citation for published version (APA):
Frigaard, P., & Brorsen, M. (1993). *A Time-Domain Method for Separating Incident and Reflected Irregular Waves*. Hydraulics & Coastal Engineering Laboratory, Department of Civil Engineering, Aalborg University.

A time-domain method for Separating Incident and Reflected Irregular Waves

Peter Frigaard & Michael Brorsen
Hydraulics & Coastal Engineering Laboratory
Aalborg University
Sohngaardsholmsvej 57, DK-9000 Aalborg, Denmark

30. august 1993

1 Introduction

In the hydraulic laboratory environment a separation of an irregular wave field into incident waves propagating towards a structure, and reflected waves propagating away from the structure is often wanted. This is due to the fact that the response of the structure to the incident waves is the target of the model test.

Goda and Suzuki (1976) presented a frequency domain method for estimation of irregular incident and reflected waves in random waves. Mansard and Funke (1980) improved this method using a least squares technique.

In the following, a time-domain method for Separating the Incident waves and the Reflected Waves (SIRW-method), is presented. The method is based on the use of digital filters and can separate the wave fields in *real time*.

2 Principle

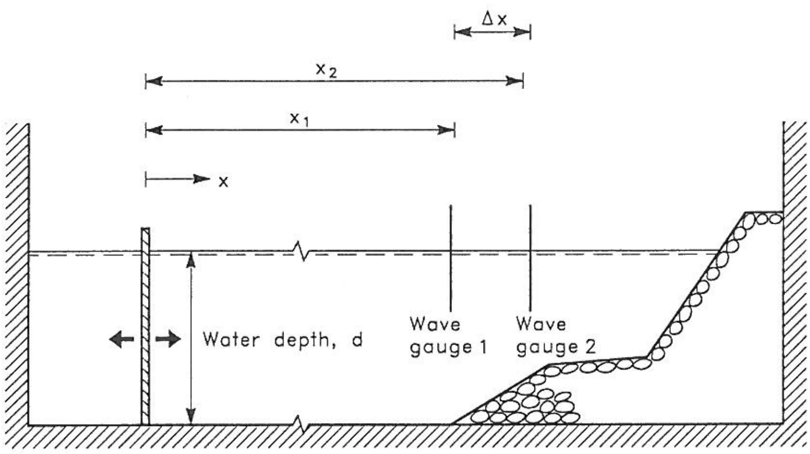

Figure 1: *Wave channel with piston-type wave generator.*

To illustrate the principle of the SIRW-method the set-up shown in Fig. 1 will be considered. The surface elevation $\eta(x,t)$ at a distance x from the wave generator may be written as the sum of the incident and reflected waves. The incident wave propagating away from the wave generator, and the reflected wave propagating towards the wave generator. Even though the method works for irregular waves it will be demonstrated in the following pages for the case of monochromatic waves.

$$\begin{aligned}\eta(x,t) &= \eta_I(x,t) + \eta_R(x,t) \\ &= a_I cos(2\pi ft - kx + \phi_I) + a_R cos(2\pi ft + kx + \phi_R) \qquad (1)\end{aligned}$$

where

f	: frequency
$a = a(f)$	: wave amplitude
$k = k(f)$	: wave number
$\phi = \phi(f)$	: phase

and indices I and R denote incident and reflected, respectively.

At the two wave gauges we have:

$$\eta(x_1,t) = a_I cos(2\pi ft - kx_1 + \phi_I) + a_R cos(2\pi ft + kx_1 + \phi_R) \qquad (2)$$

$$\begin{aligned}\eta(x_2,t) &= a_I cos(2\pi ft - kx_2 + \phi_I) + a_R cos(2\pi ft + kx_2 + \phi_R) \\ &= a_I cos(2\pi ft - kx_1 - k\Delta x + \phi_I) + \\ &\quad a_R cos(2\pi ft + kx_1 + k\Delta x + \phi_R) \qquad (3)\end{aligned}$$

where $x_2 = x_1 + \Delta x$ has been substituted into eq. (3).
It is seen that the incident wave is phaseshifted $\Delta\phi = k\Delta x$ from signal $\eta(x_1, t)$ to signal $\eta(x_2, t)$, and the reflected wave is phaseshifted $\Delta\phi = -k\Delta x$ due to opposite travel directions. These phaseshifts are called the physical phaseshifts and are denoted ϕ_I^{phys} and ϕ_R^{phys}, respectively.

The idea in the following manipulations of the elevation signals is to phase-shift the signals from the two wave gauges in such ways that the incident parts of the wave signals are in phase while the reflected parts of the signals are in mutual opposite phase. In this case the sum of the two manipulated signals is proportional to and in phase with the incident wave signal.

An amplification C and a theoretical phase shift ϕ^{theo} are introduced into the expressions for $\eta(x, t)$. The modified signal is denoted η^*. For the i'th wave gauge signal the modified signal is defined as:

$$\begin{aligned}\eta^*(x_i,t) &= Ca_I cos(2\pi ft - kx_i + \phi_I + \phi_i^{theo}) + \\ &\quad Ca_R cos(2\pi ft + kx_i + \phi_R + \phi_i^{theo})\end{aligned} \tag{4}$$

This gives at wave gauges 1 and 2:

$$\begin{aligned}\eta^*(x_1,t) &= Ca_I cos(2\pi ft - kx_1 + \phi_I + \phi_1^{theo}) + \\ &\quad Ca_R cos(2\pi ft + kx_1 + \phi_R + \phi_1^{theo})\end{aligned} \tag{5}$$

$$\begin{aligned}\eta^*(x_2,t) &= Ca_I cos(2\pi ft - kx_2 + \phi_I + \phi_2^{theo}) + \\ &\quad Ca_R cos(2\pi ft + kx_2 + \phi_R + \phi_2^{theo}) \\ &= Ca_I cos(2\pi ft - kx_1 - k\Delta x + \phi_I + \phi_2^{theo}) + \\ &\quad Ca_R cos(2\pi ft + kx_1 + k\Delta x + \phi_R + \phi_2^{theo})\end{aligned} \tag{6}$$

The sum of $\eta^*(x_1,t)$ and $\eta^*(x_2,t)$, which is denoted $\eta^{calc}(t)$, gives:

$$\begin{aligned}\eta^{calc}(t) &= \eta^*(x_1,t) + \eta^*(x_2,t) \\ &= Ca_I cos(2\pi ft - kx_1 + \phi_I + \phi_1^{theo}) + \\ &\quad Ca_R cos(2\pi ft + kx_1 + \phi_R + \phi_1^{theo}) + \\ &\quad Ca_I cos(2\pi ft - kx_1 - k\Delta x + \phi_I + \phi_2^{theo}) + \\ &\quad Ca_R cos(2\pi ft + kx_1 + k\Delta x + \phi_R + \phi_2^{theo}) \\ &= 2Ca_I cos(0.5(-k\Delta x - \phi_1^{theo} + \phi_2^{theo})) \\ &\quad cos(2\pi ft - kx_1 + \phi_I + 0.5(-k\Delta x + \phi_1^{theo} + \phi_2^{theo})) + \\ &\quad 2Ca_R cos(0.5(-k\Delta x + \phi_1^{theo} - \phi_2^{theo})) \\ &\quad cos(2\pi ft + kx_1 + \phi_R + 0.5(k\Delta x + \phi_1^{theo} + \phi_2^{theo}))\end{aligned} \tag{7}$$

It is seen that $\eta^{calc}(t)$ and $\eta_I(x_1, t) = a_I cos(2\pi f t - kx_1 + \phi_I)$ are identical signals in case:

$$
\begin{aligned}
&2C cos(0.5(-k\Delta x - \phi_1^{theo} + \phi_2^{theo})) = 1 && (8)\\
&0.5(-k\Delta x + \phi_1^{theo} + \phi_2^{theo}) = n \cdot 2\pi \qquad n \in (0, \pm 1, \pm 2, ..) && (9)\\
&0.5(-k\Delta x + \phi_1^{theo} - \phi_2^{theo}) = \frac{\pi}{2} + m \cdot \pi \qquad m \in (0, \pm 1, \pm 2, ..) && (10)
\end{aligned}
$$

Solving eq (8) - eq (10) with respect to $\phi_1^{theo}, \phi_2^{theo}$ and C gives eq (11) - eq (13). n and m can still be chosen abitrarily.

$$
\begin{aligned}
\phi_1^{theo} &= k\Delta x + \pi/2 + m\pi + n2\pi && (11)\\
\phi_2^{theo} &= -\pi/2 - m\pi + n2\pi && (12)\\
C &= \frac{1}{2cos(-k\Delta x - \pi/2 - m\pi)} && (13)
\end{aligned}
$$

All the previous considerations and calculations were done in order to find an amplification and a phaseshift for each of the two elevation signals η_1 and η_2.

Eq (11) - eq (13) gives the result of our efforts, i. e. $\eta_I(x_1, t) = \eta^{calc}(t)$. Remembering that $\phi_1^{theo} = \phi_1^{theo}(f), \phi_2^{theo} = \phi_2^{theo}(f)$ and $C = C(f)$ it is seen that the goal is already reached in *frequency domain.* However, the implementation of the principle will be done in *time domain* using digital filters.

It is seen that singularities may occur. The consequences and the handling of the singularities will be treated later on in the paper. Here it should just be mentioned that one way to bypass the singularities is to use a velocity meter instead of one of the two wave gauges. Nevertheless, this paper will concentrate on using elevation signals from two wave gauges.

$$
\begin{tikzcd}
\eta(x_1,t) \arrow[r] & \boxed{\text{FILTER 1}} \arrow[dr] & & \\
& & \oplus \arrow[r] & \eta_I(x_1,t) \\
\eta(x_2,t) \arrow[r] & \boxed{\text{FILTER 2}} \arrow[ur] & &
\end{tikzcd}
$$

Figure 2: *Flow diagram for signals in the SIRW-method.*

The purposes of the filters shown in Fig. 2 are exactly a frequency dependent amplification and a frequency dependent phaseshift on each of the two elevation signals.

Taking $n = 0$ and $m = 0$ the frequency response functions $H_1(f)$ for filter 1 and $H_2(f)$ for filter 2 calculated due to eq (8) - eq (11) are given below in complex notation:

$$
\begin{aligned}
Re\{H_1(f)\} &= \frac{1}{2cos(-k\Delta x - \pi/2)} \cdot cos(k\Delta x + \pi/2) \\
Im\{H_1(f)\} &= \frac{1}{2cos(-k\Delta x - \pi/2)} \cdot sin(k\Delta x + \pi/2) \qquad (14) \\
Re\{H_2(f)\} &= \frac{1}{2cos(-k\Delta x - \pi/2)} \cdot cos(-\pi/2) \\
Im\{H_2(f)\} &= \frac{1}{2cos(-k\Delta x - \pi/2)} \cdot sin(-\pi/2) \qquad (15)
\end{aligned}
$$

Based on eq (14) and (15) it is straight forward to design the time domain filters. The design of the filters will be given on the next pages.

3 Design of filters

The impulse response of the filters is found by an inverse *discrete* Fourier transformation, which means that N discrete values of the complex frequency response are used in the transformation, see Fig. 3.

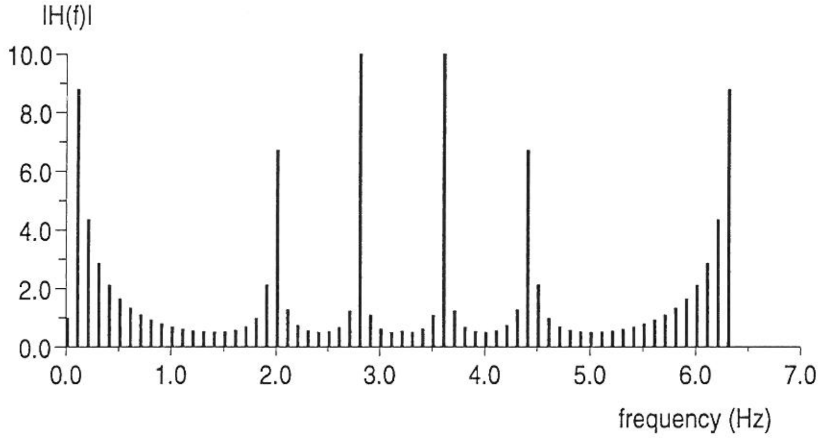

Figure 3: *Magnitude (gain) of the frequency responses of a discrete filter.* $N = 64$, $d = 0.5\ m$, $\Delta f = 0.10\ Hz$, $\Delta t_{filter} = 0.16\ sec.$, $\Delta x = 0.2m$.

This gives an impulse response of *finite* duration, i.e. the impulse response h^j or the filter coefficients are found by:

$$h^j = h(j \cdot \Delta t_{filter}) = \sum_{r=0}^{N-1} H^r \cdot e^{i\frac{2\pi r j}{N}} \tag{16}$$

where

r = 0,..., N-1
j = 0,..., N-1

and H^r is the complex frequency response given by eq (14) and (15) at the frequency $f = r \cdot \Delta f$.

The frequency increment, Δf, in the frequency response is found by

$$\Delta f = \frac{1}{N \cdot \Delta t_{filter}} \tag{17}$$

where Δt_{filter} is the time increment of the filter.

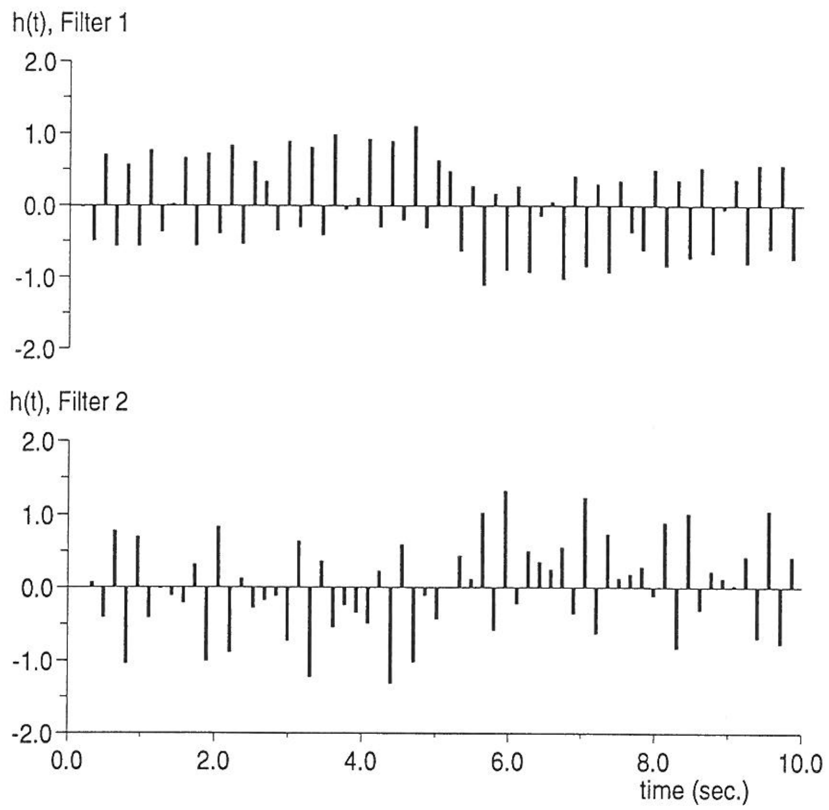

Figure 4: *Filter coefficients corresponding to Filter 1 and Filter 2.* $N = 64$ *, waterdepth = 0.5 m,* Δf*=0.10 Hz,* Δt_{filter} *= 0.16 sec.,*$\Delta x = 0.2m$.

The price paid for handling only N frequencies in this transformation, is a minor inaccuracy in the performance of the filter at input frequencies, which do not coincide with one of the calculated frequencies in the discrete filter.

If the length of the filter (N) is increased, more frequencies are included, and in principle the overall accuracy of the filter is improved. In practice, however, there is a limit beyond which the accuracy of the filter starts to decrease due to other effects in the model.

The *convolution* integral (summation), eq (18), describes the input-output relationship for the filters. Notice, that it can be shown from eq (18) that the output $\eta^*(x,t)$ is delayed N/2-1 time steps relative to the input $\eta(x,t)$.

$$\eta^{*p} = \sum_{j=0}^{N-1} h^j \cdot \eta^{p-j} \tag{18}$$

where

j,p = 0,..., N-1
η^{p-j} : elevation at time $t = (p-j) \cdot \Delta t_{filter}$
η^{*p} : output from filter at time $t = p \cdot \Delta t_{filter}$
h^j : the filter coefficient corresponding to time $t = j \cdot \Delta t_{filter}$

Fig. 3 indicates that in the present example, singularities are present at frequencies of app. 2.0 Hz and 2.8 Hz. The figure also shows that due to the fact that the frequency response is calculated only at *discrete frequencies* in the filters, the singularities will not *destroy* the calculations. However, it is recommended to *cut off* the frequency responses whenever the value is larger than app. 5-10. For practical use this means that, if $|H(f)| \geq 5$ when calculated, then $|H(f)|$ should be valued 5. Furthermore, it is recommended to *place* the singularities in a frequency range where the wave spectrum is without significant energy. This can always be done by choosing appropriate values of Δx and Δt_{filter}.

4 Results

NUMERICAL EXAMPLES

In order to evaluate the SIRW-method we will look at two numerical examples with known incident and reflected waves. The error is described by the difference between the calculated incident wave signal η^{calc} and the actual incident wave signal η_I.

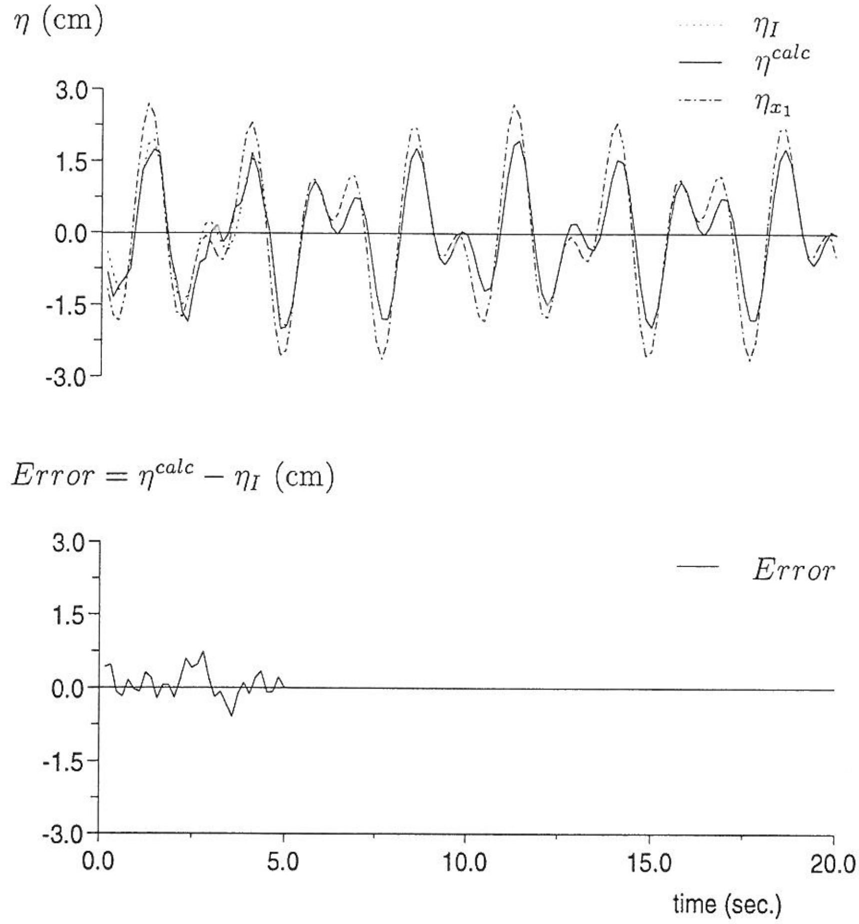

Figure 5: *A comparison between* η_I, η^{calc} *and* η_{x_1}.
$f_1 = 4\Delta f$, $f_2 = 7\Delta f$.

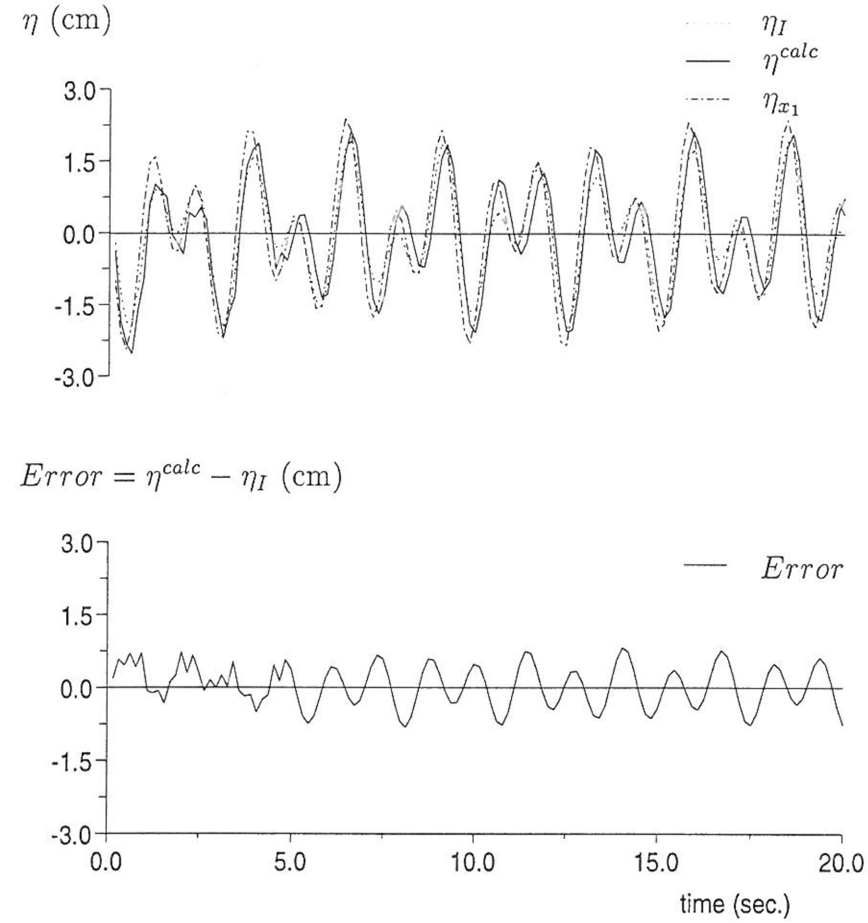

Figure 6: *A comparison between* η_I, η^{calc} *and* η_{x_1}.
$f_1 = 4.2\Delta f$, $f_2 = 7.5\Delta f$.

In the examples the total elevation is described by eq (19), corresponding to 50 % reflection of the incident waves.

$$\begin{aligned}\eta(x,t) &= 0.01 \cdot cos(2\pi f_1 t - k_1 x) + 0.01 \cdot cos(2\pi f_2 t - k_2 x) + \\ &\quad 0.01 \cdot 0.5 \cdot cos(2\pi f_1 t + k_1 x) + \\ &\quad 0.01 \cdot 0.5 \cdot cos(2\pi f_2 t + k_2 x) \end{aligned} \tag{19}$$

The signals are sampled with a frequency of 6.4 Hz. Fig. 5 illustrates the functionality of the method, when f_1 and f_2 both are coinciding with some

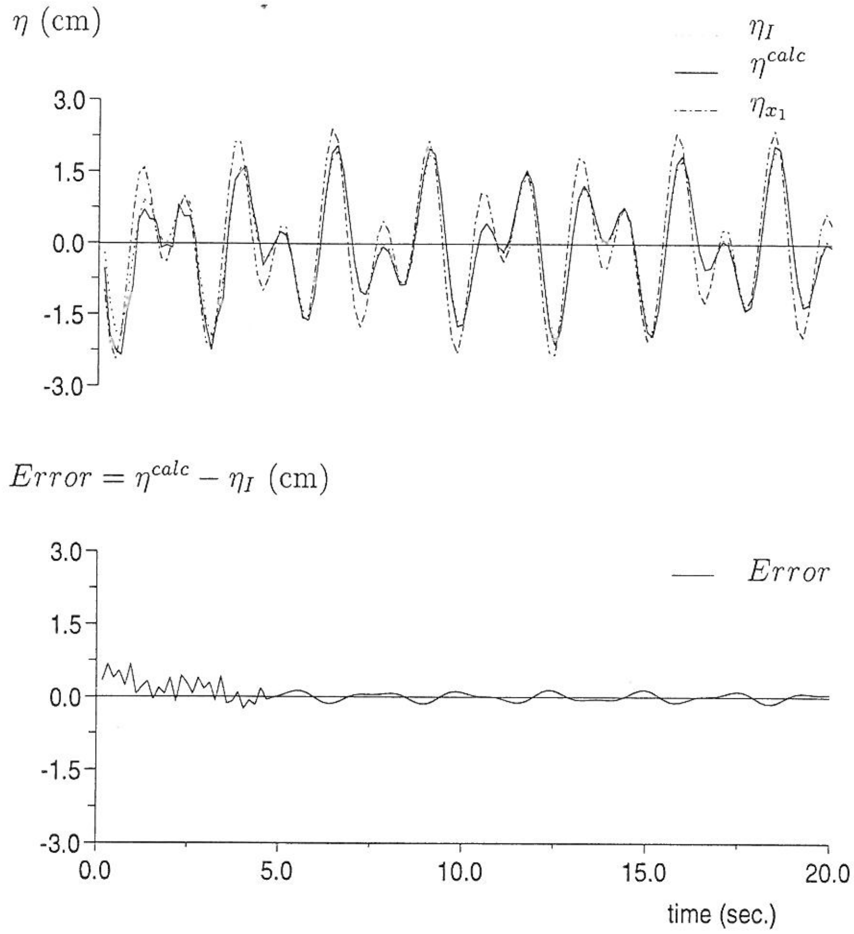

Figure 7: *A comparison between η_I, η^{calc} and η_{x_1}. The filters have been cosine tapered.* $f_1 = 4.2\Delta f$, $f_2 = 7.5\Delta f$.

frequencies of the discrete filter, i.e. $n \cdot \Delta f$. As expected the method is exact for signals only consisting of energy placed at the discrete frequencies (Fig. 5), though it is seen that errors are present during *warm up* of the filters.

The second example (Fig. 6) is identical to the first example except that f_1 and f_2 are not coinciding with frequencies in the digital filter i.e. $f_1 = 4.2\Delta f$, $f_2 = 7.5\Delta f$.

It must be stressed that the output signal shown in Fig. 6 corresponds to the worst case situation, where the wave frequencies are placed midway between filter frequencies. One way to improve the results is to apply a tapering of the filter coefficients, because the output from a digital filter is more stable in case the absolute values of the filter coefficients are almost zero in both ends of the filter, Karl (1989). Cosine tapering of the filter coefficients improves the accuracy of the SIRW method as demonstrated in Fig. 7.

PHYSICAL MODEL TESTS

The SIRW-method previously described were also tested in a laboratory flume at the Hydraulics and Coastal Engineering Laboratory, Aalborg University, cf Fig 8.

First, the waves (incident part of the timeseries) given by eq (19) were generated and sent towards a spending permeable beach (slope 1:8) in order to obtain a good estimate of the incident waves. Next, a reflecting wall were mounted in the flume giving a fairly high reflection (app. 50 %) and the same incident waves were reproduced by play back of the same digital steering signal to the wave maker.

In Fig. 9 the output from the SIRW-filters is compared with the incident waves measured in case of very low reflection.

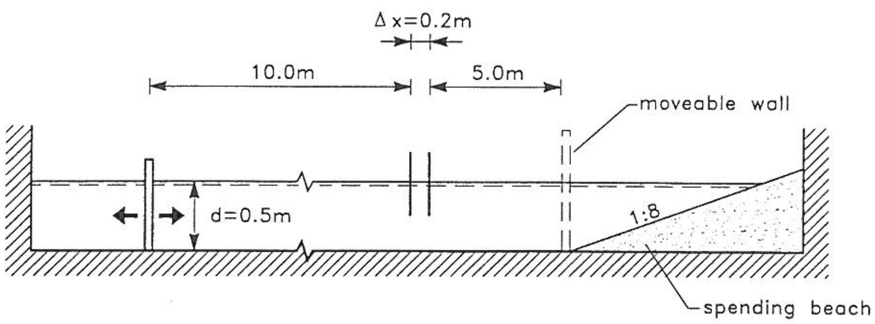

Figure 8: *Set-up for physical model tests.*

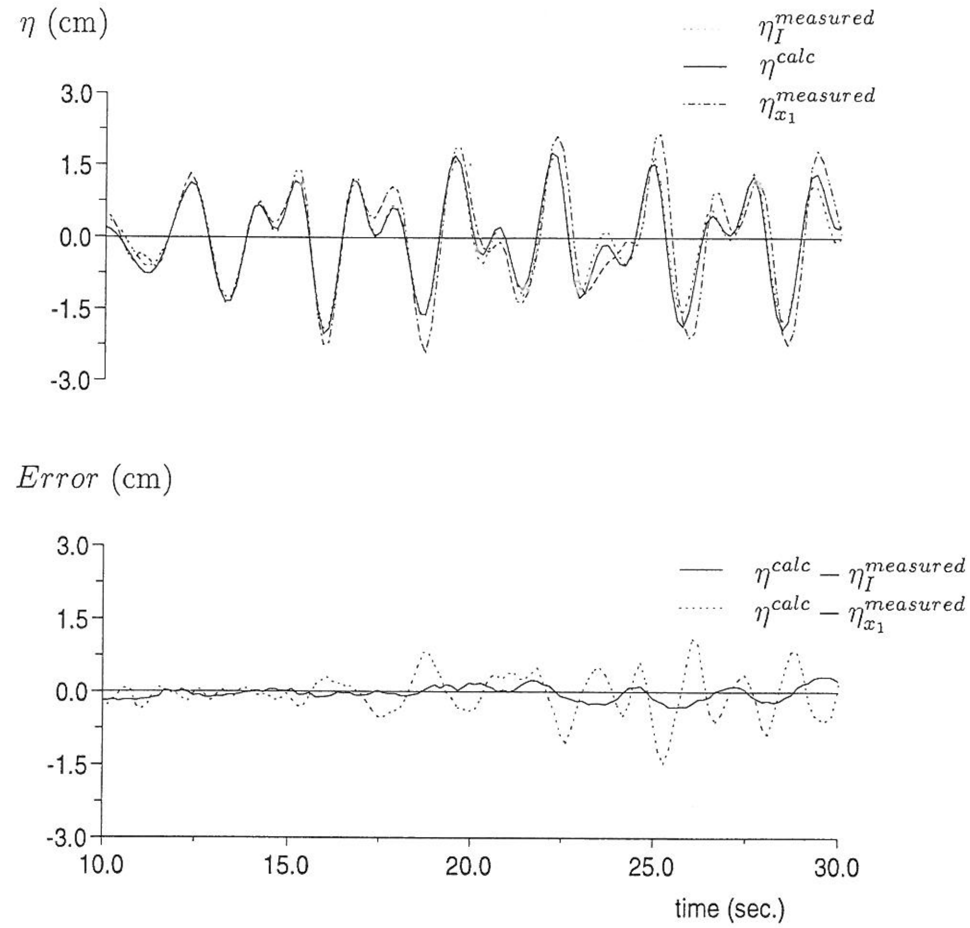

Figure 9: *A comparison between* $\eta_I^{measured}$, η^{calc} *and* $\eta_{x_1}^{measured}$. $f_1 = 4.2\Delta f$, $f_2 = 7.5\Delta f$.

The specific part of the signals, where reflection is present but re-reflection from the wave paddle is still not present, is shown. In the the specific example the SIRW-method reduces the error (variance) from 30 % of the incident energy to 3 % of the incident energy.

5 Conclusions

A time-domain method for Separating Incident and Reflected Irregular Waves (The SIRW-method) has been presented.

By numerical and physical model tests it is demonstrated that the method is quite efficient in separating the total wave field into incident and reflected waves. Please note, that all the tests shown were done with fairly small filters (few filter components), and that longer filters will improve the efficiency of the method. Taking the example shown in Fig. 6 and doubling the number of filter coefficients the error (variance) will decrease to 2/3 of the shown example.

The accuracy of the SIRW-method is comparable with the accuracy of the method proposed by Goda and Suzuki (1976), but the SIRW-method has the advantage that in case the incident wave signal is wanted in *time domain* (i.e. for zero-crossing analysis) the singularity points are treated more properly than in the Goda-method. The SIRW-method can easily be extended to give same accuracy as the method proposed by Mansard and Funke (1980).

Though, the largest advantage of the SIRW-method is that it works in *real time*. Brorsen and Frigaard (1992) used digital filters to make a new open boundary condition in a Boundary Element Model, based on a filtering of the surface elevation. The boundary condition accumulated errors, because separation of the surface elevation into incident and reflected waves were not possible in *real time* at that moment and, consequently, the Boundary Element Model could only run for some time.

At the moment the SIRW-method is implemented at Aalborg Hydraulics Laboratory, Aalborg University and the method is used in a project dealing with active absorption. Results from this research will be published in the near future.

6 References:

Brorsen, M. and Frigaard, P., 1992.
"Active Absorption of Irregular Gravity Waves in BEM-models"
Boundary Elements XIV, Vol.1
Editors: Brebbia, Dominiquez and Paris. Computational Mechanics Publications, Southampton.

Goda, Y. and Suzuki, Y., 1976.
"Estimation of Incident and Reflected Waves in Random Wave Experiments"
Proceedings, 15th International Conference on Coastal Engineering, Vol. 1, pp. 828-845, Honolulu, Hawaii.

Karl, John H., 1989.
"An Introduction to Digital Signal Processing"
Academic Press, San Diego.

Mansard, E. and Funke, E., 1980.
"The Measurement of Incident and Reflected Spectra Using a Least Squares Method"
Proceedings, 17th International Conference on Coastal Engineering, Vol. 1, pp 154-172, Sydney, Australia.